Electronic Structure of $Ru_2(O_2CR)_4^+$ and $Rh_2(O_2CR)_4^+$ Complexes

Joe G. Norman, Jr.,*†[1a] George E. Renzoni,[1a] and David A. Case[1b]

Contribution from the Department of Chemistry, University of Washington, Seattle, Washington 98195, and the Department of Chemistry, University of California, Davis, California 95616. *Received March 13, 1979*

Abstract: SCF-Xα-SW calculations of $Ru_2(O_2CH)_4Cl_2^-$, $Ru_2(O_2CH)_4^+$, $Ru_2(O_2CH)_4$, $Rh_2(O_2CH)_4(H_2O)_2^+$, and $Rh_2(O_2CH)_4^+$ are used to discuss the bonding, magnetic properties, stable oxidation level, axial ligand trans influence, electronic spectra, and ESR spectra of ruthenium and rhodium carboxylate dimers. The Ru(2.5) dimers are predicted to have a $\sigma^2\pi^4\delta^2\pi^{*2}\delta^{*1}$ configuration, corresponding to three unpaired electrons as found by experiment. For the Rh(2.5) dimers, the predicted configuration is $\sigma^2\pi^4\delta^2\pi^{*4}\delta^{*1}$. Reasons for the close spacing of π^* and δ^* orbitals, and the energy order $\pi^* < \delta^*$, are discussed. Favorable exchange energy and susceptibility of the Ru(II) dimer to Jahn-Teller distortion are seen as factors stabilizing the Ru(2.5) oxidation level. An explanation is given for the observed changes in Rh-Rh, Rh-OH_2, and Rh-O(acetate) distances between $Rh_2(O_2CR)_4(H_2O)_2$ and $Rh_2(O_2CR)_4(H_2O)_2^+$. Comparison of $Ru_2(O_2CH)_4Cl_2^-$ and $Rh_2(O_2CH)_4(H_2O)_2^+$ indicates that Cl^- is slightly better than H_2O at weakening a trans metal-metal bond. The observed order of Rh-Rh distances in $Rh_2(O_2CCH_3)_4L_2$, L = H_2O, py, $NHEt_2$, CO, PR_3, is interpreted as consistent with the Xα-SW energy level diagram. The prominent band near 2 μm^{-1} in the visible spectrum of $Ru_2(O_2CR)_4^+$ complexes is assigned to an $O\pi \rightarrow \pi^*$ transition, where "$O\pi$" is a mainly Ru-O orbital, but with significant Ru-Ru π character. The weak band near 1 μm^{-1} in the aqueous solution spectrum is assigned to mainly the $\delta \rightarrow \delta^*$ transition. The bands near 1.9 and 2.5 μm^{-1} in the acidic solution spectrum of $Rh_2(O_2CCH_3)_4(H_2O)_2^+$ are assigned to $\pi^* \rightarrow \sigma^*$ and $\pi^* \rightarrow$ Rh-O σ^* transitions, respectively, as for the analogous bands of $Rh_2(O_2CCH_3)_4(H_2O)_2$. The extra band which appears for the cation near 1.3 μm^{-1} is tentatively assigned to the $\delta \rightarrow \delta^*$ transition. Good agreement is obtained between calculated and experimental g values for the Ru(2.5) dimers. Problems in developing a suitable model for calculation of hyperfine coupling constants are discussed.

A significant fraction of our efforts to provide accurate theoretical models for metal-metal bonded compounds[2-7] is directed toward the dinuclear carboxylates $M_2(O_2CR)_4L_2$, which have idealized D_{4h} symmetry when the carboxylate substituents R are planar and the axial ligands L are linear. These have been structurally characterized for a wide variety of metals, namely, M = V^{2+}, Cr^{2+}, Co^{2+}, Cu^{2+}, Mo^{2+}, Tc^{3+}, $Ru^{2.5+}$, $Rh^{2+,2.5+}$, and Re^{3+}.[8-16] They are thus convenient for studying the variation of metal-metal bonding and metal-metal/metal-ligand bond interactions with M and L for a constant cis ligand framework. We have previously analyzed such questions, and assigned photoelectron and electronic spectra, using SCF-Xα-SW calculations of $Mo_2(O_2CH)_4$,[3] $Rh_2(O_2CH)_4$,[5] and $Rh_2(O_2CH)_4(H_2O)_2$.[5] Others have similarly treated $Cr_2(O_2CH)_4$,[17] and an SCF-HF-LCAO treatment of $Cr_2(O_2CH)_4$, $Mo_2(O_2CH)_4$, and $CrMo(O_2CH)_4$ has recently appeared.[18] The combination of the calculations and sophisticated experimental investigations of structures and spectra[19,20] has greatly increased our understanding of these important compounds.

The $Ru^{2.5+}$ carboxylates are well characterized in the solid state as $[Ru_2(O_2CR)_4]Cl$, with axial chloride ions bridging two $Ru_2(O_2CR)_4$ units as depicted in **1**,[14a,21] and very recently as $Ru_2(O_2CR)_4Cl_2^-$ and $Ru_2(O_2CR)_4(H_2O)_2^+$, also depicted in **1**.[14b] The Ru-Ru distances lie between those in $Mo_2(O_2CCH_3)_4$ (2.09 Å)[13] and $Rh_2(O_2CCH_3)_4(H_2O)_2$ (2.39 Å),[15a] where our calculations[3,5] indicate quadruple and single metal-metal bonds, respectively. The Ru-Cl bonds are sufficiently weak that the chloro compounds are 1:1 electrolytes in aqueous solution,[21a] reflecting the strong trans influence of the metal-metal bond,[22] which we have discussed in some detail for rhodium(II) carboxylates.[5] These compounds are unique among the strongly metal-metal bonded carboxylate dimers in having the $M_2(O_2CR)_4$ unit stable as a 1+ ion, so that the average metal oxidation state is nonintegral, and in having three unpaired electrons per dimer.[21a,23] By contrast, their Mo, Tc, Rh, and Re analogues are most stable with neutral or dipositive $M_2(O_2CR)_4$ units, and are all diamagnetic. Attempts to reduce $Ru_2(O_2CR)_4^+$ by one electron[21b,23,24] lead only to ill-characterized products or decomposition. A good comparison is with the rhodium system, where $Rh_2(O_2CCH_3)_4^+$ can be prepared under special conditions[24,25] and indeed even the crystal structure of $[Rh_2(O_2CCH_3)_4(H_2O)_2]ClO_4 \cdot H_2O$ has been determined,[15c] but the ion easily reverts to the air-stable neutral complex.

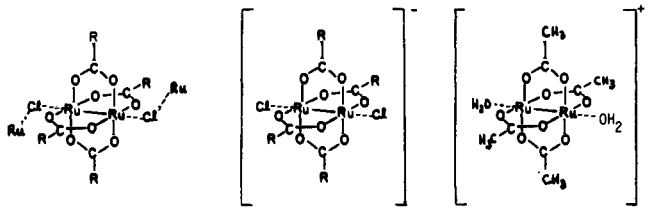

Ru-Ru = 2.27 (R = CH_3), 2.28 (R = C_3H_7) 2.29 (R = C_2H_5), Ru-Cℓ = 2.57 (R = CH_3), 2.59 (R = C_3H_7), 2.57 (R = C_2H_5)

Ru-Ru = 2.29 Ru-Cℓ = 2.52 (R = H, CH_3)

Ru-Ru = 2.25 Å Ru-OH_2 = 2.27, 2.34 Å

1

These unusual properties have stimulated several experimental investigations of the electronic structure responsible for them. The electronic spectra in aqueous solution (where the species is probably $Ru_2(O_2CR)_4(H_2O)_2^+$) have been reported from the near-infrared to the ultraviolet region,[21a,24] and compared with the spectra of $Rh_2(O_2CR)_4(H_2O)_2^{0,+}$ and the ephemeral one-electron-reduced Ru compound.[24] The diffuse-reflectance spectra of solid $[Ru_2(O_2CR)_4]Cl$ were described in conjunction with a resonance-Raman study which concluded that the prominent visible absorption near 500 nm is due to a dipole-allowed electronic transition.[26] Frozen solution EPR spectra of $Ru_2(O_2CC_3H_7)_4Cl$ were used to derive g values and ^{99}Ru hyperfine coupling constants.[23] However, no accurate theoretical calculations have been reported to help interpret these data. The original proposal of a $\sigma^2\pi^4\delta^2\sigma_n{}^1\sigma_n{}'^1\delta^{*1}$ ground state,[14a] with the high-spin character arising from close spacing of the σ_n, σ_n', and δ^* orbitals, now seems untenable: all the recent theoretical and experimental work

† Fellow of the Alfred P. Sloan Foundation, 1978-1980.

0002-7863/79/1501-5256$01.00/0

Table II. Total Energies, Xα Exchange Energies, and Virial Ratios[a]

	E_T	$V_{X\alpha}$	$-2T/V$
$Ru_2(O_2CH)_4$	−9638.9298	−350.3963	1.000 25
$Ru_2(O_2CH)_4^+$	−9638.8432	−350.1234	1.000 21
$Ru_2(O_2CH)_4Cl_2^-$	−10 558.1267	−406.1765	1.000 30
$Rh_2(O_2CH)_4$	−10 127.0066	−359.8986	1.000 30
$Rh_2(O_2CH)_4^+$	−10 126.8449	−359.5743	1.000 27
$Rh_2(O_2CH)_4(H_2O)_2$	−10 280.9064	−378.4538	1.000 11
$Rh_2(O_2CH)_4(H_2O)_2^+$	−10 280.7146	−378.3331	1.000 13

[a] Spin-polarized results in hartrees. Note that these quantities do depend on choice of bond lengths and sphere radii; see Computational Section for details of these choices.

on related systems indicates that the σ_n and σ_n' orbitals (essentially nonbonding $p_z d_{z^2}$ hybrids directed outward from the ends of the metal-metal axis) are much too high in energy to be occupied.

In this paper we offer detailed explanations for the preferred oxidation level and magnetic properties of ruthenium carboxylate dimers, based on comparative SCF-Xα-SW calculations of $Ru_2(O_2CH)_4Cl_2^-$, $Ru_2(O_2CH)_4^+$, $Ru_2(O_2CH)_4$, $Rh_2(O_2CH)_4(H_2O)_2^+$, and $Rh_2(O_2CH)_4^+$. We have briefly noted our essential conclusion about the ground-state electronic configuration of $Ru_2(O_2CR)_4^+$ in our previous paper on $Rh_2(O_2CH)_4(H_2O)_2$, $Rh_2(O_2CH)_4$, and Rh_2.[5] The comparison of $Ru_2(O_2CH)_4Cl_2^-$ and $Ru_2(O_2CH)_4^+$ also allows analysis of the interactions between the Ru-Ru and Ru-Cl bonds, thus providing a second theoretical picture of the metal-metal trans influence. The calculations on $Rh_2(O_2CH)_4(H_2O)_2^+$, compared with those on $Rh_2(O_2CH)_4(H_2O)_2$, allow analysis of the observed[15a,c] differences in bond lengths between $[Rh_2(O_2CCH_3)_4(H_2O)_2]ClO_4 \cdot H_2O$ and $Rh_2(O_2CCH_3)_4(H_2O)_2$. We also comment in this context on the recent[15b] structures of $Rh_2(O_2CCH_3)_4L_2$, L = py, $NHEt_2$, CO, PR_3, giving an interpretation of the observed Rh-Rh and Rh-L variation differing from that in the structural paper.

Our calculations lead to an assignment of the electronic spectra of $Ru_2(O_2CR)_4^+$ complexes which differs from those previously proposed,[14a,24,26] and to the first assignment of the twice-reported[24,25] spectrum of $Rh_2(O_2CR)_4^+$ in solution. We anticipate eventual tests of both assignments by single-crystal polarized spectra;[27] if correct, they bring some new perspective to the continuing discussion[20] of $\delta \rightarrow \delta^*$ transitions in D_{4h} dimers. We have also calculated ESR parameters for $Ru_2(O_2CH)_4Cl_2^-$, using the Xα-SW properties package,[28] for comparison with experiment.

Computational Section

Coordinates for $Ru_2(O_2CH)_4Cl_2^-$, $Ru_2(O_2CH)_4^+$, and $Ru_2(O_2CH)_4$ in atomic units were derived from the average crystallographic bond parameters[14] of $[Ru_2(O_2CC_3H_7)_4]Cl$, namely, Ru-Ru = 2.28, Ru-Cl = 2.59, Ru-O = 2.00, C-O = 1.27, and C-H = 1.08 Å and Ru-Ru-O angle = 89.3°, using the relation 1 bohr = 0.529 17 Å and D_{4h} symmetry. For $Rh_2(O_2CH)_4(H_2O)_2^+$ Rh-Rh = 2.32, Rh-OH_2 = 2.31, and Rh-O = 2.01 Å were taken from the crystal structure[15c] of $[Rh_2(O_2CCH_3)_4(H_2O)_2]ClO_4 \cdot H_2O$. Other dimensions and the H_2O orientation were as for $Rh_2(O_2CH)_4(H_2O)_2$.[5] Dimensions for $Rh_2(O_2CH)_4^+$ were as for $Rh_2(O_2CH)_4$;[5] we were unaware of the structure of $[Rh_2(O_2CCH_3)_4(H_2O)_2]ClO_4 \cdot H_2O$ at this time. Overlapping atomic sphere radii were obtained nonempirically,[29] as 91% of the atomic-number radii, except for $Rh_2(O_2CH)_4^+$, where 89.3% was used. Touching outer-sphere radii were employed. Sphere radii and SCF charges in the various regions are summarized in Table I (available as supplementary material).

In other respects the calculations were carried out as for $Mo_2(O_2CH)_4$.[3b] For $Ru_2(O_2CH)_4Cl_2^-$, spherical harmonics through $l = 1$ were used on Cl, and a 1+ "Watson sphere"[30] was used to simulate the stabilizing effect of the surrounding crystal lattice. Both spin-restricted and spin-polarized ground-state SCF calculations were done for all species, since all were expected to be paramagnetic. Spin-polarized transition-state calculations of electronic transition energies were carried out for $Ru_2(O_2CH)_4Cl_2^-$ and $Rh_2(O_2CH)_4(H_2O)_2^+$. The SCF potential for $Ru_2(O_2CH)_4Cl_2^-$, together with estimates of electronic transition energies, was used to calculate ESR parameters for $Ru_2(O_2CH)_4Cl_2^-$.

Results

The energy level diagrams, as for other $M_2(O_2CH)_4$ species,[3b,5] contain three distinct regions. Twenty essentially unperturbed formate C-H and C-O σ orbitals lie in the ranges −1.25 to −0.65 hartree for $Ru_2(O_2CH)_4^+$ and $Rh_2(O_2CH)_4(H_2O)_2^+$ and −1.10 to −0.50 hartree for Watson-sphere stabilized $Ru_2(O_2CH)_4Cl_2^-$. Mainly C-O π, metal-O σπ, and O nonbonding orbitals follow next in energy, intermixed with primarily metal-metal orbitals; the highest occupied orbitals are always partially filled mainly metal-metal π* and δ*. There is a large energy gap between these and the completely empty orbitals, which are, in order of increasing energy, mainly metal-metal σ*, metal-O σ* (two orbitals), and C-O π* (four orbitals). For $Ru_2(O_2CH)_4Cl_2^-$ and $Rh_2(O_2CH)_4(H_2O)_2^+$, additional orbitals correlating best with the σ and π lone pairs of Cl^- and H_2O, respectively, are found in the second region, those for Cl^- lying about 0.12 hartree higher relative to the $M_2(O_2CH)_4$ levels than those for H_2O.

Table II compares the total energies, exchange energies, and virial ratios for the calculated SCF ground states of all species. The first excited state for $Ru_2(O_2CH)_4$, $5e_g^2 2b_{1u}^2$, is particularly close to the $5e_g^3 2b_{1u}^1$ ground state; the calculated separation in total energy is only ca. 2 kcal/mol. Energies and charge distributions for upper valence levels are given in Table III for $Ru_2(O_2CH)_4^+$ and $Ru_2(O_2CH)_4Cl_2^-$, and in Table IV for $Rh_2(O_2CH)_4(H_2O)_2^+$. Figure 1 compares the energy levels of $Ru_2(O_2CH)_4$, $Ru_2(O_2CH)_4^+$, and $Ru_2(O_2CH)_4Cl_2^-$, with emphasis on those important for Ru-Ru and Ru-Cl bonding. Figure 2 presents a similar comparison for $Rh_2(O_2CH)_4(H_2O)_2$ and $Rh_2(O_2CH)_4(H_2O)_2^+$. Wave function contour maps comparing important metal-metal and metal-(axial ligand) orbitals of $Ru_2(O_2CH)_4Cl_2^-$ and $Rh_2(O_2CH)_4(H_2O)_2^+$ appear in Figures 3-5. Our assignment for the electronic spectra of $Ru^{2.5+}$ and $Rh^{2.5+}$ carboxylates appears in Tables V and VI, respectively.

Discussion

Magnetic Properties of Ru Carboxylates. As shown in Figure 1, the predicted Ru-Ru bond order in $Ru_2(O_2CH)_4^+$ and $Ru_2(O_2CH)_4Cl_2^-$ is 2.5. The three unpaired electrons observed experimentally[23] are also predicted explicitly by the spin-polarized calculations. The high-spin, $S = {}^3/_2$ $e_g^2 b_{1u}^1$ ($\pi^{*2}\delta^{*1}$) configuration is favored over $S = {}^1/_2$ alternatives by close spacing of the π* and δ* orbitals. We now examine reasons for this close spacing, and for the related fact that the δ* level lies slightly higher in energy than the π* level for these Ru and Rh carboxylates.

The ordering $\delta^* < \pi^*$ is expected if metal-metal bonding entirely determines it. Consistently, we find this ordering in Rh_2 and Rh_2^{4+}, where only metal-metal bonds are present,[5] and in $Mo_2(O_2CH)_4$, where the Mo-Mo bonding is so strong that it dominates other factors.[3] We see three factors interacting to produce the inversion in the Ru and Rh carboxylates: (1) downward shift of metal 4d levels relative to ligand levels from Mo to Ru to Rh; (2) influence of the carboxylate ligands; (3) influence of the axial ligands. Let us eliminate (3) for the

Table III. Spin-Restricted Upper Valence Levels (hartrees)[a] and Charge Distributions for $Ru_2(O_2CH)_4^+$ and $Ru_2(O_2CH)_4Cl_2^-$

$Ru_2(O_2CH)_4^+$						$Ru_2(O_2CH)_4Cl_2^-$						
D_{4h} level	energy	% charge[b] 2Ru	% charge[b] $4O_2CH$	major Ru basis fns[c]	main type	D_{4h} level	energy	% charge[b] 2Ru	% charge[b] $4O_2CH$	% charge[b] 2Cl	major Ru basis fns[c]	main type
$2a_{2g}$	+0.0025		100		C-O π*	$2a_{2g}$	−0.0043		100			C-O π*
$3b_{2g}$	−0.0201	4	96			$4b_{2g}$	−0.0065	4	96			
$7e_u$	−0.0176	0	100			$9e_u$	−0.0206	0	97	2		
$5b_{1g}$	−0.0870	59	41	$d_{x^2-y^2}$	Ru-O σ*	$5b_{1g}$	−0.0846	61	39		$d_{x^2-y^2}$	Ru-O σ*
$4b_{2u}$	−0.1029	66	34	$d_{x^2-y^2}$*		$4b_{2u}$	−0.0992	67	33		$d_{x^2-y^2}$*	
$4a_{2u}$	−0.1627	84	16	d_{z^2}*	Ru-Ru σ*	$6a_{2u}$	−0.1140	75	12	12	d_{z^2}*	Ru-Ru σ*, Ru-Cl σ*
$2b_{1u}$[d]	−0.2250	69	31	d_{xy}*	Ru-Ru δ*	$2b_{1u}$[d]	−0.2214	71	29		d_{xy}*	Ru-Ru δ*
$5e_g$[d]	−0.2347	89	11	$d_{xz,yz}$*	Ru-Ru π*	$6e_g$[d]	−0.2224	85	6	9	$d_{xz,yz}$*	Ru-Ru π*
						$7a_{1g}$	−0.2421	23	5	72	d_{z^2}, p_z	Ru-Cl σ*, Ru-Ru σ
$2b_{2g}$	−0.2672	84	16	d_{xy}	Ru-Ru δ	$2b_{2g}$	−0.2621	85	15		d_{xy}	Ru-Ru δ
						$7e_u$	−0.2653	16	8	76		
						$5e_g$	−0.2755	6	8	86		Cl π lone pair
						$5a_{2u}$	−0.2891	9	9	82	d_{z^2},* s*, p_z*	Ru-Cl σ
$6e_u$	−0.2860	30	70	$d_{xz,yz}$, $p_{x,y}$	Ru-O π	$6e_u$	−0.2924	24	56	20	$d_{xz,yz}$, $p_{x,y}$	Ru-O π
$1a_{1u}$	−0.3013		100		O lone pair	$1a_{1u}$	−0.3046		100			O lone pair
$4e_g$	−0.3104	8	92			$4e_g$	−0.3141	7	89	4		
$3e_g$	−0.3246	6	94			$3e_g$	−0.3272	5	94	1		
$5e_u$	−0.3389	71	29	$d_{xz,yz}$	Ru-Ru π	$5e_u$	−0.3385	63	34	3	$d_{xz,yz}$	Ru-Ru π
$5a_{1g}$	−0.3286	42	58	s, d_{z^2}	Ru-O σ, Ru-Ru σ	$6a_{1g}$	−0.3416	27	57	16	s, d_{z^2}	Ru-O σ, Ru-Cl σ
$3a_{2u}$	−0.3549	18	82	d_{z^2}*, s*	Ru-O σ, π	$4a_{2u}$	−0.3595	19	75	6	d_{z^2}*, s*	Ru-O σ, Ru-Ru σ*
$3b_{2u}$	−0.3662	21	79	$d_{x^2-y^2}$*		$3b_{2u}$	−0.3687	20	80		$d_{x^2-y^2}$*	Ru-O σ, π
$1b_{1u}$	−0.3821	37	63	d_{xy}*		$1b_{1u}$	−0.3808	34	66		d_{xy}*	
$4b_{1g}$	−0.3885	34	66	$d_{x^2-y^2}$		$4b_{1g}$	−0.3927	33	67		$d_{x^2-y^2}$	
$1a_{2g}$	−0.3921		100		C-O π	$1a_{2g}$	−0.3957		100			C-O π
$4a_{1g}$	−0.3976	73	27	d_{z^2}	Ru-Ru σ, Ru-O σ	$5a_{1g}$	−0.4029	66	24	10	d_{z^2}	Ru-Ru σ, Ru-O σ
$4e_u$	−0.4104	2	98		C-O π	$4e_u$	−0.4131	1	99	0		C-O π
$1b_{2g}$	−0.4513	19	81	d_{xy}	Ru-OC π	$1b_{2g}$	−0.4517	17	83		d_{xy}	Ru-OC π

[a] All levels above −0.5 hartree except for diffuse Rydberg-state orbitals. These occur for $Ru_2(O_2CH)_4Cl_2^-$ at −0.0758 ($8a_{1g}$), −0.0644 ($8e_u$), −0.0580 ($7a_{2u}$), −0.0554 ($3b_{2g}$), −0.0360 ($7e_g$), −0.0217 ($6b_{1g}$), −0.0183 ($9a_{1g}$), and −0.0123 ($3b_{1u}$). Only 3-10% of their charge is located within the atomic spheres; 0.15 hartree has been added to the actual $Ru_2(O_2CH)_4^+$ eigenvalues to make the 20 formate-localized orbitals below −0.5 hartree essentially coincident in the two complexes. [b] *Relative* amounts of charge within the atomic spheres. The only $Ru_2(O_2CH)_4Cl_2^-$ orbitals with less than 77% of the total charge within the atomic spheres are the unoccupied $9e_u$, $4b_{2g}$, and $2a_{2g}$ (35-57%). [c] Spherical harmonics contributing more than 10% of the Ru charge for important Ru-Ru, Ru-Cl, and Ru-O_2CH orbitals, listed in order of decreasing importance. All such Ru contributions are more than 80% d except for the following: $Ru_2(O_2CH)_4Cl_2^-$, $6a_{1g}$ (67% s, 30% d_{z^2}) and $7a_{1g}$ (68% d_{z^2}, 24% p_z); $Ru_2(O_2CH)_4^+$, $5a_{1g}$ (52% s, 42% d_{z^2}). Asterisks indicate antibonding combinations, no asterisks bonding combinations. [d] Half-occupied levels. Those below are completely filled, those above completely empty. In the spin-polarized calculation for $Ru_2(O_2CH)_4Cl_2^-$, the occupied $2b_{1u}\uparrow$ and $6e_g\uparrow$ are 66% Ru and 74% Ru/20% Cl, respectively, while the empty $2b_{1u}\downarrow$ and $6e_g\downarrow$ are 74% Ru and 89% Ru/6% Cl, respectively. Other orbitals with more than 10% difference between the spin-up and -down Ru contributions are $5a_{1g}$ (↑72%, ↓61%), $1b_{1u}$ (↑41%, ↓30%), $5e_u$ (↑74%, ↓53%), and $7e_u$ (↑8%, ↓23%).

moment, and emphasize (1) and (2), by comparing in sequence the calculated energy level diagrams for $Mo_2(O_2CH)_4$, $Ru_2(O_2CH)_4$, $Ru_2(O_2CH)_4^+$, $Rh_2(O_2CH)_4(H_2O)_2$, and $Rh_2(O_2CH)_4(H_2O)_2^+$ (ref 2 and Figures 1 and 2), using the $6b_{2g}$ level for the last two to represent the π* energy ($6b_{3g}$ interacts with the axial H_2O π lone pairs).

The essential point is that the δ* d-orbital combination interacts significantly with lower lying carboxylate orbitals, while the π* does not. The $1b_{1u}$ orbital (in D_{4h}; $5b_{1u}$ for D_{2h}) is one of the eight mainly ligand orbitals which best correlate with the eight metal-oxygen bonds;[3b] its metal character is 14, 27, 37, 37, and 45% along the above series (ref 2b and Tables III and IV). By contrast the $3e_g$ and $4e_g$ orbitals (in D_{4h}; $3,4b_{3g}$ and $4,5b_{2g}$ in D_{2h}) are best identified with oxygen lone pairs; their metal character varies from 1-2% in $Mo_2(O_2CH)_4$ to 11-16% in $Rh_2(O_2CH)_4(H_2O)_2^+$. Thus, as the metal 4d *atomic* orbitals drop in energy along the sequence Mo^{2+}, Ru^{2+}, $Ru^{2.5+}$, Rh^{2+}, $Rh^{2.5+}$, the *molecular* orbital best classified as metal-metal δ* does not drop as fast as π*, because unlike π* it is the antibonding orbital of a significant metal-*carboxylate* interaction. A good single illustration of this point is the comparative δ* and π* energies for $Ru_2(O_2CH)_4$ and $Ru_2(O_2CH)_4^+$ in Figure 1.

The influence of the axial ligands is the opposite of the carboxylates. The π* rather than the δ* orbitals are destabilized more by interaction with ligand orbitals. The important lower lying ligand orbitals are the pπ lone pairs of Cl^- and H_2O; some are of π*, but none are of δ*, symmetry. Thus, as shown in Figures 1 and 2, and in Figure 1 of ref 5, the addition of axial ligands decreases the δ*-π* splitting in the Ru and Rh dimers. In no case do the calculations predict a restoration of the ordering $\delta^* < \pi^*$, but the resulting splittings are quite small, and the theory could well be in error by such amounts.

Finally, there is a related effect of metal-metal distance on the δ*-π* splitting. This is shown by the energy level diagrams for $Cr_2(O_2CH)_4$ at 2.20 and 2.36 Å;[17] the $\delta^* < \pi^*$ ordering at the shorter distance is reversed at the longer. Presumably

Table IV. Spin-Restricted Upper Valence Levels (hartrees)[a] and Charge Distribution for $Rh_2(O_2CH)_4(H_2O)_2^+$

D_{2h} level	energy	% charge[b] 2Rh	$4O_2CH$	$2H_2O$	major Rh[c] basis fns	main type
$7b_{1g}$	+0.0278	0	100			C-O π*
$9b_{2u}$	+0.0171					
$9b_{3u}$	+0.0168	1	98	1		
$11a_g$	−0.0090	4	96	0		
$6b_{1g}$	−0.0930	55	45		d_{xy}	Rh-O σ*
$5a_u$	−0.1116	62	38		d_{xy}*	
$8b_{1u}$	−0.1291	74	15	10	d_{z^2}*	Rh-Rh σ*, Rh-OH_2 σ*
$7b_{1u}$[d]	−0.2231	63	37	0	$d_{x^2-y^2}$*	Rh-Rh δ*
$6b_{3g}$	−0.2258	65	7	29	d_{yz}*	Rh-Rh π*
$6b_{2g}$	−0.2390	83	17	0	d_{xz}*	
$7b_{2u}$	−0.2451	16	17	67		H_2O π lone pair
$5b_{3g}$	−0.2651	17	30	53		
$9a_g$	−0.2640	47	17	36	d_{z^2}, s, p_z	Rh-OH_2 π*, Rh-Rh σ
$8a_g$	−0.2646	81	18	2	$d_{x^2-y^2}$	Rh-Rh δ
$7b_{3u}$	−0.2646	21	79	0	d_{xz}, p_x	Rh-O π
$6b_{2u}$	−0.2716	9	70	22		
$4a_u$	−0.2770		100			O lone pair
$5b_{2g}$	−0.2882	11	89	0		
$4b_{3g}$	−0.2913	14	79	8		
$4b_{2g}$	−0.3033	11	88	0		
$3b_{3g}$	−0.3041	16	83	2		
$6b_{1u}$	−0.3226	9	70	21	s*, d_{z^2}*	Rh-O σ
$6b_{3u}$	−0.3225	80	19	1	d_{xz}	Rh*- Rh π
$5b_{2u}$	−0.3270	78	18	4	d_{yz}	
$7a_g$	−0.3320	15	64	21	s, d_{z^2}	Rh-O σ, π
$3a_u$	−0.3476	25	75		d_{xy}*	
$5b_{1u}$	−0.3615	45	55	0	$d_{x^2-y^2}$*	
$5b_{1g}$	−0.3648	39	61		d_{xy}	
$4b_{1g}$	−0.3669	0	100			C-O π
$4b_{1u}$	−0.3694	22	13	65	d_{z^2}, p_z*	Rh-OH_2 σ, Rh-Rh σ*
$5b_{3u}$	−0.3852					
$4b_{2u}$	−0.3852	2	98	0		C-O π
$6a_g$	−0.4098	59	5	36	d_{z^2}	Rh-Rh σ, Rh-OH_2 σ
$5a_g$	−0.4260	22	78	0	d_{xy}	Rh-OC π

[a] All levels above −0.48 hartree except for diffuse Rydberg-state orbitals, which occur at −0.0252 ($10a_g$), −0.0119 ($8b_{3u}$), −0.0118 ($8b_{2u}$), −0.0056 ($9b_{1u}$), +0.0221 ($7b_{2g}$), and +0.0224 ($7b_{3g}$). Only 5-11% of their charge is located within the atomic spheres. 0.15 hartree has been added to all actual eigenvalues to make the 20 formate localized orbitals below −0.48 hartree essentially coincident with those in $Rh_2(O_2CH)_4(H_2O)_2$ and $Ru_2(O_2CH)_4Cl_2^-$. [b] *Relative* amounts of charge within the atomic spheres. The only orbitals with less than 83% of the charge there are unoccupied $7b_{1g}$, $9b_{2u}$, $9b_{3u}$, and $11a_g$ (27-63%). [c] Spherical harmonics contributing more than 10% of the Rh charge for important Rh-Rh, Rh-OH_2, and Rh-O_2CH orbitals, listed in order of decreasing importance. All such Rh contributions are more than 78% d except for $7a_g$ (59% s, 41% d_{z^2}) $6b_{1u}$ (60% s*, 40% d_{z^2}*), and $9a_g$ (69% d_{z^2}, 16% s, 15% p_z). Asterisks indicate antibonding and no asterisks bonding combinations. [d] Half-occupied level. Those below are completely filled, those above completely empty. In the spin-polarized calculation, the occupied $7b_{1u}\uparrow$ is 62% Rh and the empty $7b_{1u}\downarrow$ 64% Rh. The only orbital with more than 5% difference between the spin-up and -down Rh contributions is $6b_{3g}$ ($\uparrow$ 61% Rh/33% H_2O, $\downarrow$ 68% Rh/25% H_2O).

the reason is increasing Cr-O bond strength. The stronger the Cr-O bonds, the greater the destabilization of δ* relative to π*.

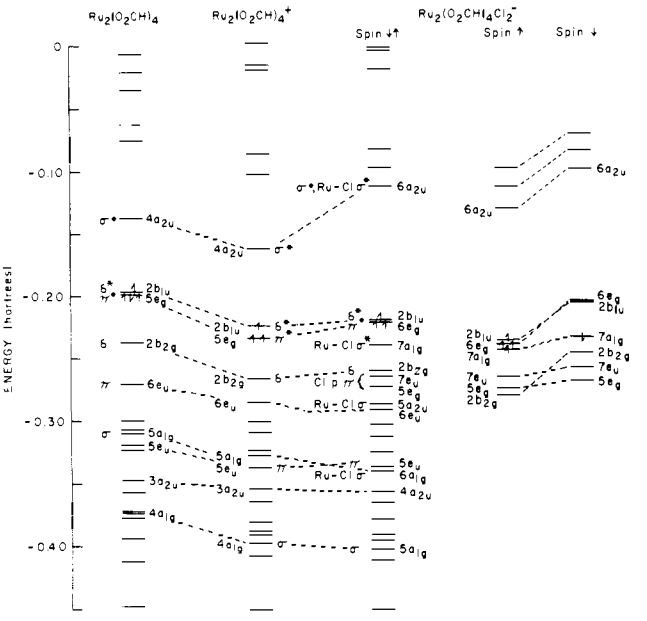

Figure 1. Spin-restricted SCF energy levels for $Ru_2(O_2CH)_4$, $Ru_2(O_2CH)_4^+$, and $Ru_2(O_2CH)_4Cl_2^-$ above −0.51 hartree, and the highest occupied and lowest unoccupied spin-polarized levels for the last. The levels best described as Ru-Ru σ, π, δ, δ*, π*, and σ*, Ru-Cl σ and σ*, and Cl pπ lone pairs are indicated. Mulliken symbols are given for these levels, and for all others of Ru-Ru σ, π, π*, and σ* symmetry (a_{1g}, e_u, e_g, and a_{2u}, respectively). The occupation of the highest filled or partially filled levels is shown.

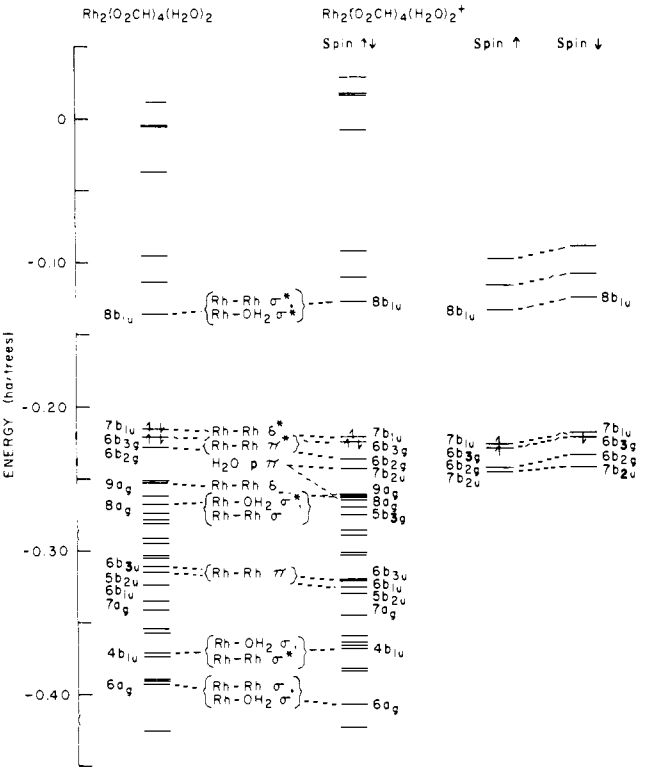

Figure 2. Spin-restricted SCF energy levels for $Rh_2(O_2CH)_4(H_2O)_2$ and $Rh_2(O_2CH)_4(H_2O)_2^+$ above −0.48 hartree, and the highest occupied and lowest unoccupied spin-polarized levels for the latter. The levels best described as Rh-Rh σ, π, δ, δ*, π*, and σ*, Rh-OH_2 σ and σ*, and H_2O pπ lone pairs are indicated. Mulliken symbols are given for these levels, and for all others of Rh-Rh σ and σ* symmetry (a_g and b_{1u}, respectively). The occupation of the highest filled or partially filled levels is shown.

The conclusion of general value from this analysis, which could not have been reached without the calculations, is that for these weaker metal-metal bonds the relative ordering of

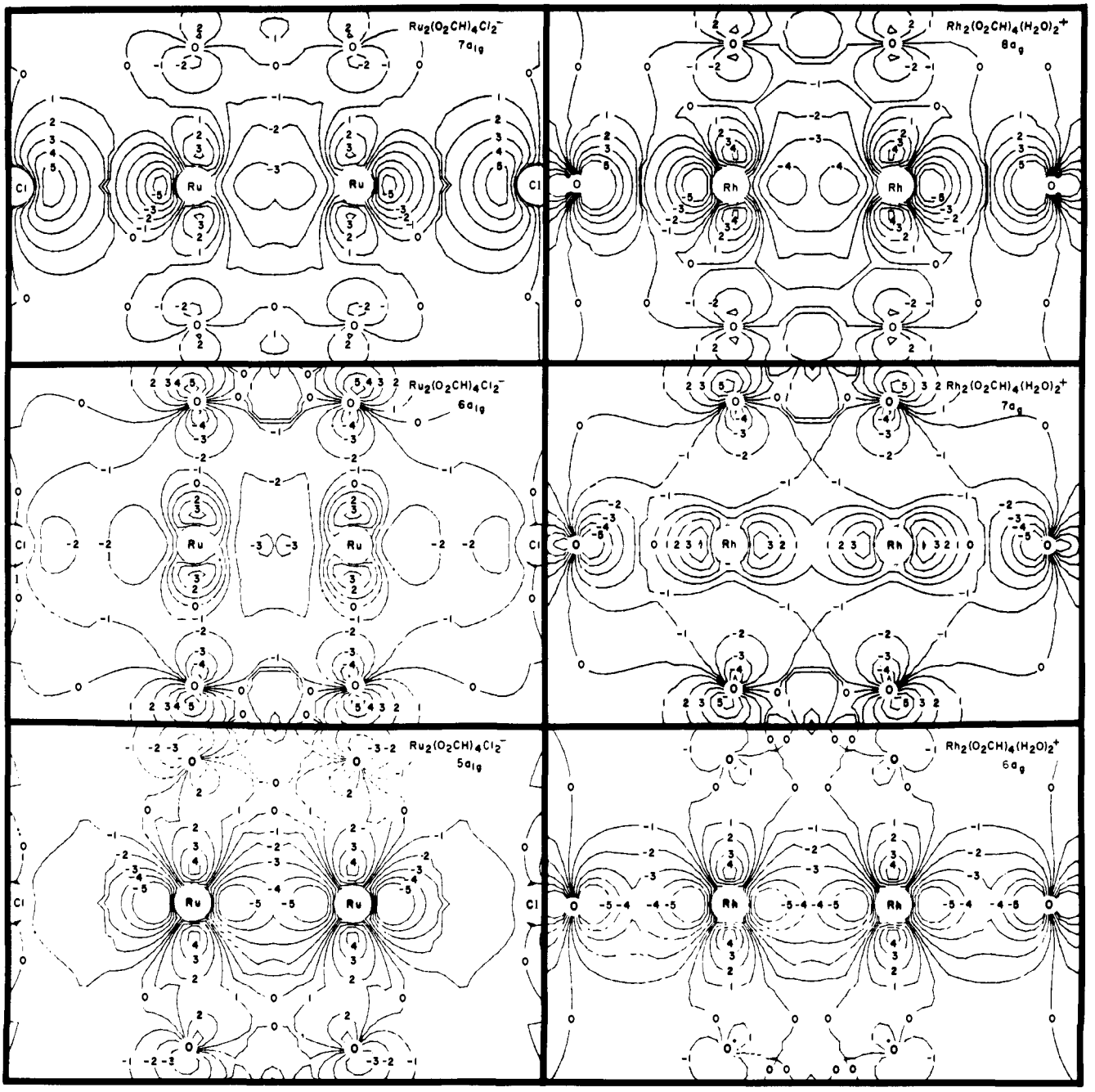

Figure 3. Contour maps of the wave functions for the important metal–metal σ orbitals of $Ru_2(O_2CH)_4Cl_2^-$ and $Rh_2(O_2CH)_4(H_2O)_2^+$, showing the bonding of the trans ligands in a_{1g}/a_g symmetry. These maps and those of Figure 4 and the left half of Figure 5 are in the plane of two of the formate groups. For Figures 3–5 the contour values are 0, ±1, ±2, ±3, ±4, ±5 = 0, ±0.02, ±0.09, ±0.13, ±0.17, respectively, and inner contours close to the atomic centers are omitted for clarity.

π^* and δ^*, and their exact separation, is greatly influenced by the ligands present. In other words, $Ru^{2.5}$–$Ru^{2.5}$ D_{4h} dimers with other ligands might well have a different net spin and orbital occupation. Recently, the first such compounds, $Ru_2(N_4C_{22}H_{22})_2^{0,+,2+}$, have been characterized.[31] The ligand is a tetradentate macrocycle and the crystal structure of the $Ru^{2.5+}$ ion shows a nonbridged, approximately D_{4h} dimer with Ru–Ru = 2.26 Å (cf. 2.25–2.29 Å in the carboxylates). The 0, 1+, and 2+ species contain two, one, and zero unpaired electrons, respectively. As the authors of ref 31 point out, the reasonable electronic configurations implied by this data are $\delta^{*2}\pi^{*2}$, $\delta^{*2}\pi^{*1}$, and $\delta^{*1}\pi^{*0}$, respectively. The conclusion is that the δ^* level lies considerably below π^* in this case.

Stable Oxidation Level of Ru and Rh Carboxylates. Any half-filled set of degenerate orbitals has special stability relative to surrounding configurations, since this is a favorable situation for exchange energy. The calculations thus suggest that one major contribution to the stability of $Ru_2(O_2CR)_4^+$ relative to $Ru_2(O_2CR)_4$ is the half-filled π^* set attained in the former (see Figure 1). There is no such stabilizing factor for $Rh_2(O_2CR)_4^+$ relative to $Rh_2(O_2CR)_4$, since the two extra electrons added from Ru to Rh fill the π^* orbital completely (see Figure 2). We have explicitly verified this suggestion by comparing exchange energies and total energies of $M_2(O_2CH)_4^{0,+}$, M = Ru, Rh (see Table II). The positive ion is indeed predicted to be much more stable relative to the neutral species in the Ru case, and about $^2/_3$ of the extra stability can be traced to the exchange energy.

The other point to be made in this connection is that the neutral Ru species is predicted to be susceptible to Jahn–Teller

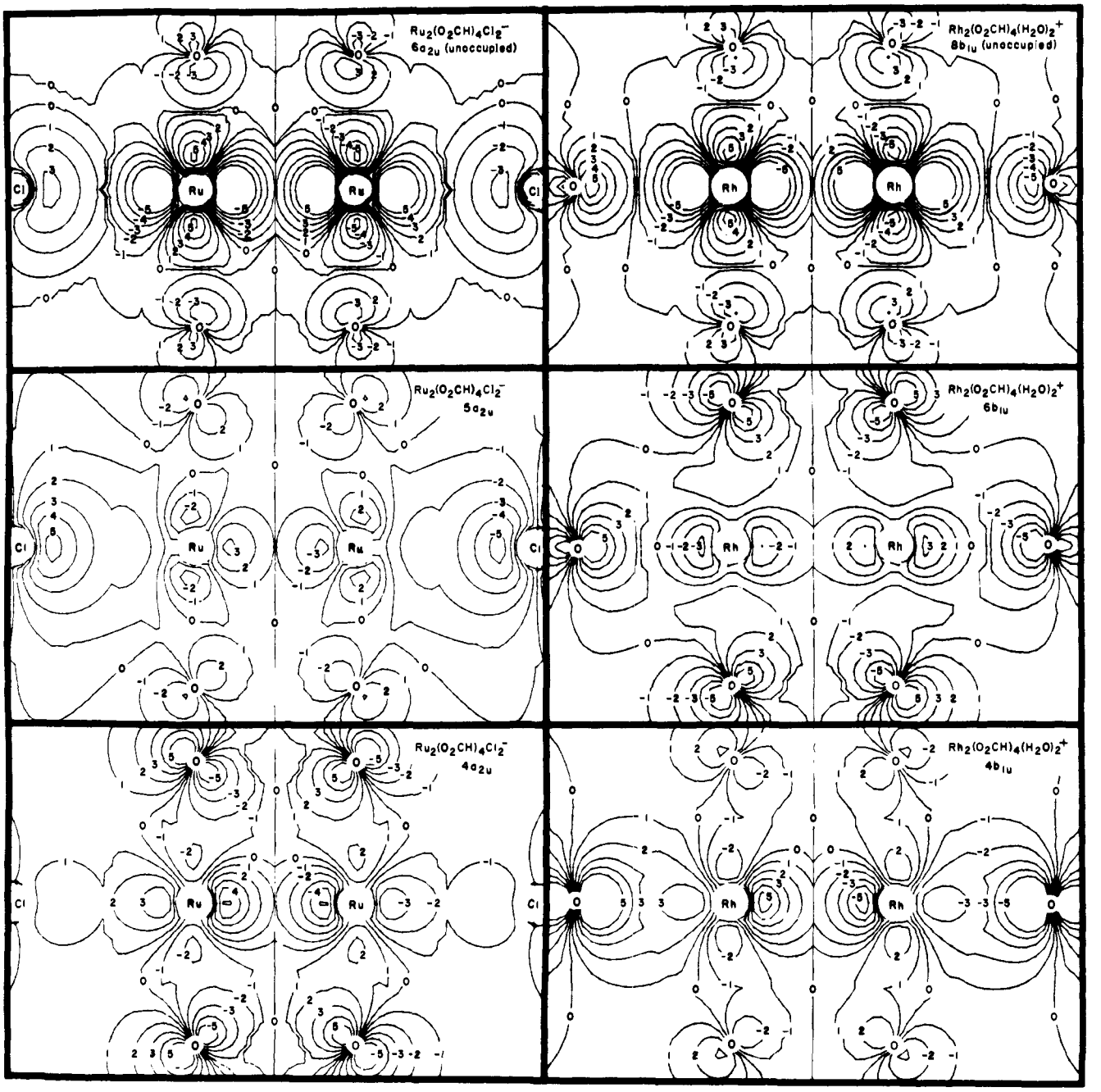

Figure 4. Contour maps of the wave functions for the important metal-metal σ^* orbitals of $Ru_2(O_2CH)_4Cl_2^-$ and $Rh_2(O_2CH)_4(H_2O)_2^+$, showing the bonding of the trans ligands in a_{2u}/b_{1u} symmetry.

distortion (see Figure 1). This would take the form of elongation of Ru-O distances in one plane and shortening in the other. The neutral species would thereby become more thermodynamically stable, but perhaps also more reactive toward decomposition of the cage structure. The neutral species prepared by electrochemical reduction of the cation in solution is indeed observed to decompose at an appreciable rate.[23]

These ideas suggest an explanation for the unusual conditions required for success in the original synthesis of $Ru_2(O_2CR)_4Cl$. Although the overall reaction was a reduction from Ru^{3+} in $RuCl_3$ to $Ru^{2.5+}$ in the dimer, an *oxygen* atmosphere was necessary to obtain a good yield.[21a] Possibly the role of O_2 is to keep ruthenium from being reduced below oxidation state 2.5, so as to avoid the irreversible decomposition of the cage structure. A newer synthesis[21b] uses excess Cl^- in place of O_2, which again should stabilize $Ru_2(O_2CR)_4^+$ relative to $Ru_2(O_2CR)_4$.

$(Cl-Ru-Ru-Cl)^{3+}$ vs. $(H_2O-Rh-Rh-OH_2)^{5+}$. The four orbitals of $Ru_2(O_2CH)_4Cl_2^-$ which correlate best with the Cl^- lone pairs are, in order of increasing energy, $5a_{2u}$, $5e_g$, $7e_u$, and $7a_{1g}$ (see Figure 1). The first two have Ru-Cl bonding character, and the last two Ru-Cl antibonding character, because the lone-pair combinations of a_{2u} and e_g symmetry are lower in energy, while those of e_u and a_{1g} symmetry are higher in energy, than the Ru-Ru orbitals with which they interact (σ^*, π^*, π, and σ, respectively). The ordering reflects this difference in character, and also the fact that the Ru-Cl σ interaction (involving Ru-Ru σ and σ^* orbitals) is stronger than the Ru-Cl π interaction (involving Ru-Ru π and π^* orbitals).

We first consider whether the π interaction is important. Since the Ru-Ru π^* orbitals are only half filled, there is an opportunity for net Cl $\pi \rightarrow$ Ru-Ru π^* charge transfer, which would strengthen the Ru-Cl bonds at the expense of the Ru-Ru bond. However, the orbital overlap is small, as shown

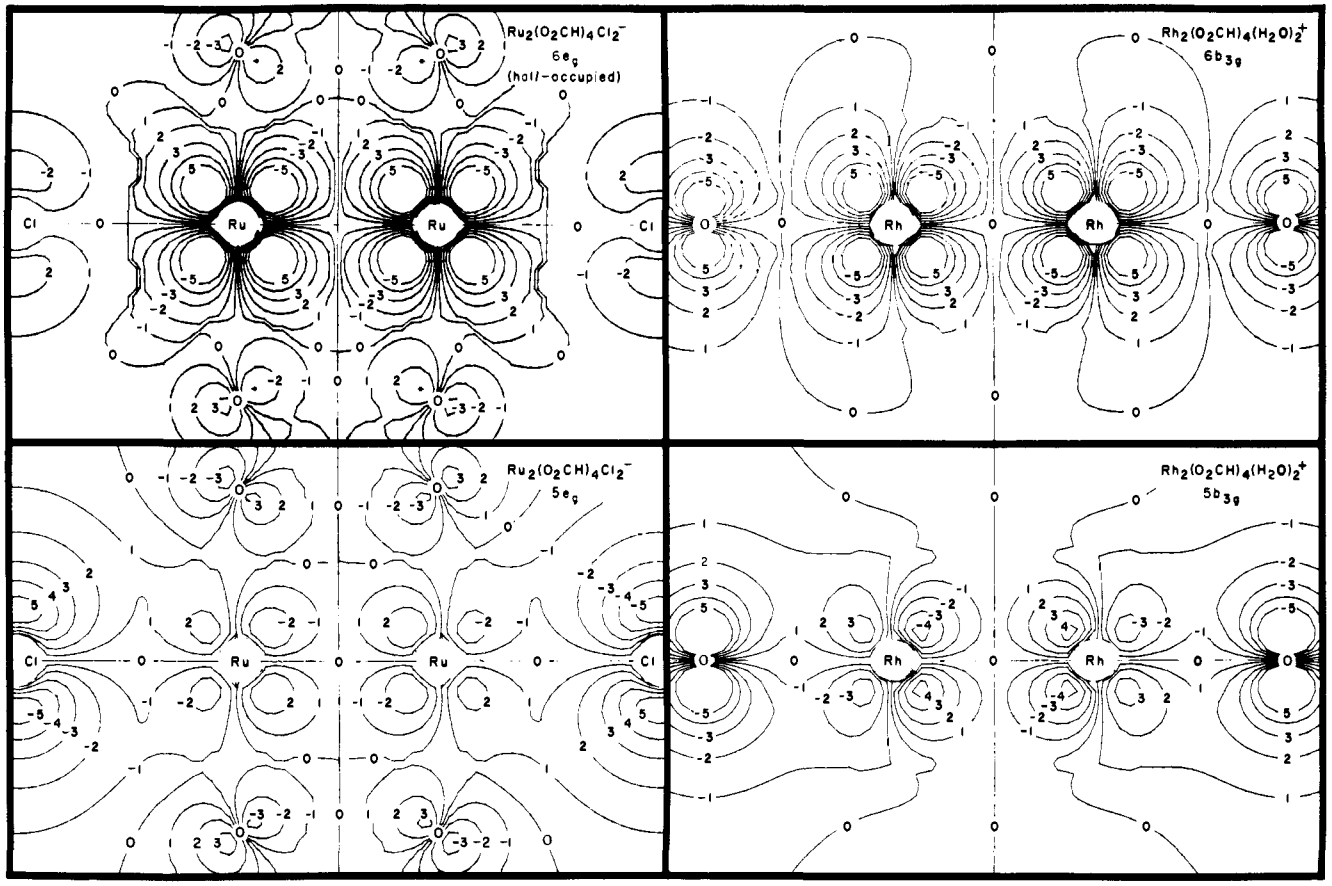

Figure 5. Contour maps of the wave functions of the important metal-metal π^* orbitals of $Ru_2(O_2CH)_4Cl_2^-$ and $Rh_2(O_2CH)_4^+$ which can interact with the $p\pi$ lone pairs of the trans ligands. The plane for the $Rh_2(O_2CH)_4(H_2O)_2^+$ maps lies halfway between those of the formate groups, and perpendicular to that of the water molecules.

in Figure 5. The Ru-Cl π overlap in $5e_g$ may be compared with the main Ru-Cl σ overlaps, which occur in $4,5a_{2u}$ (Figure 4) and arise from Cl $\sigma \rightarrow$ Ru-Ru σ^* donation. There appears to be about an order of magnitude less π than σ overlap *charge* (wave function squared). Since the Ru-Cl σ bonding is already weak compared to normal bonds, we neglect the net Ru-Cl π bonding as unimportant in our subsequent discussion of the Cl^- trans influence.

This is not to say that there is not considerable polarization of the Cl^- π lone pairs by the Ru-Ru π and π^* electrons, and vice versa. For example, the mainly-Cl $7e_u$ orbital has 16% Ru character. In $Rh_2(O_2CH)_4(H_2O)_2^+$, despite the completely filled π^* orbitals and resultant impossibility of *net* H_2O $\pi \rightarrow$ Rh-Rh π^* charge transfer, there is even more pronounced orbital mixing; e.g., the mainly Rh-Rh π^* $6b_{3g}$ orbital has 29% H_2O character. Such polarization is important in its influence on the *character* of highest occupied orbitals and molecular properties which reflect this. However, it should not be confused with bonding—i.e., with strong orbital overlap and, especially when both bonding and antibonding orbitals are filled, with net charge transfer.

The $(Cl\text{-}Ru\text{-}Ru\text{-}Cl)^{3+}$ and $(H_2O\text{-}Rh\text{-}Rh\text{-}OH_2)^{5+}$ σ systems have much in common. As for $Rh_2(O_2CH)_4(H_2O)_2$,[5] in both a_{1g}/a_g (M-M σ) and a_{2u}/b_{1u} (M-M σ^*) symmetries, the $M_2(O_2CH)_4$ unit contributes two orbitals and the axial ligand L one to the bonding. The three MOs which result in the present cases are depicted in Figure 3 for a_{1g}/a_g and Figure 4 for a_{2u}/b_{1u}. Our previous general conclusions about the mutual influence of the M-M and M-L bonds[5] apply equally well to the present cases, and will not be repeated here.

The question we wish to discuss is which ligand, Cl^- or H_2O, is more effective at weakening the M-M σ bond by trans coordination. As is evident from Figures 3 and 4, the presence of the carboxylates complicates the picture. For this reason we present in **2** interaction diagrams based on the calculations,

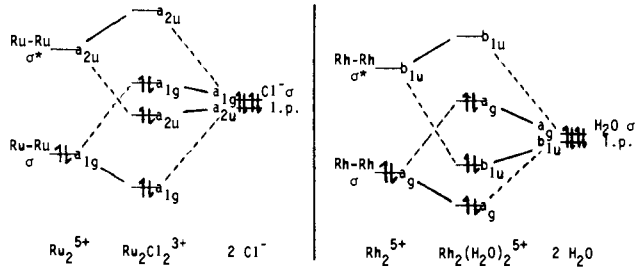

2

but simplified to omit the carboxylate orbitals. The clear difference between Cl^- and H_2O is the higher relative energy of the Cl^- σ lone pairs. This has several consequences for the M-M bond strength, which we now explore.

The important first-order M-M bond weakening upon trans ligand coordination results from ligand lone pair donation into the M-M σ^* orbital. The magnitude of the donation is reflected in the MOs by the amount of M-M σ^* character found in *filled* orbitals of a_{2u}/b_{1u} symmetry. From the diagram above, one expects Cl^- to be a more effective donor than H_2O, all other things being constant, since its lone pairs are closer in energy to the M-M σ^* orbital. However, Figure 4 indicates that the two are about equally effective in the two cases at hand. H_2O introduces more σ^* character into the lower of the two filled orbitals ($4a_{2u}$, $4b_{1u}$), but Cl^- more into the upper one ($5a_{2u}$, $6b_{1u}$). The point is that all other things are *not* constant: the $Ru^{2.5+}$-$Ru^{2.5+}$ bond is stronger, and should be harder to

Table V. Electronic Spectra of $Ru^{2.5+}$ Carboxylates (μm^{-1})

D_{4h} transition	selection rule	type[a]	Calcd,[b] $Ru_2(O_2CH)_4Cl_2^-$	exptl,[c] $[Ru_2(O_2CCH_3)_4]Cl$	exptl,[d] $Ru_2(O_2CCH_3)_4(H_2O)_2^+$
$2b_{2g} \rightarrow 6e_g$	forbidden	$\delta \rightarrow \pi^*$	0.86		0.90 } (ϵ 60)
$2b_{2g} \rightarrow 2b_{1u}$	allowed z	$\delta \rightarrow \delta^*$	0.88		1.04 }
$7e_u \rightarrow 6e_g$	allowed z	Cl $\rightarrow \pi^*$	1.35		
$5e_g \rightarrow 2b_{1u}$	allowed xy	Cl $\rightarrow \delta^*$	1.60		
$5a_{2u} \rightarrow 6e_g$	allowed xy	Cl $\rightarrow \pi^*$	1.87	1.76 sh	
$6e_u \rightarrow 6e_g$	allowed z	O$\pi \rightarrow \pi^*$	1.99	2.16	2.35 (ϵ 700)
$1a_{1u} \rightarrow 6e_g$	allowed xy	O $\rightarrow \pi^*$	2.30		
$6e_g \rightarrow 6a_{2u}$	allowed xy	$\pi^* \rightarrow \sigma^*$	2.41		
$4e_g \rightarrow 2b_{1u}$	allowed xy	O $\rightarrow \delta^*$	2.47		

[a] δ, δ^*, π^*, and σ^* denote the Ru–Ru character of mainly Ru orbitals. Cl and O denote predominantly Cl and O lone pair orbitals, respectively. Oπ is a predominantly oxygen orbital with significant (24%) Ru–Ru π character (see Table III). [b] All spin- and dipole-allowed transitions between 0.8 and 2.7 μm^{-1}, and the lowest lying spin-allowed, dipole-forbidden transition in this range, from spin-polarized calculations. [c] Band maxima in diffuse reflectance spectrum of solid (ref 26), from 1.4 to 3.2 μm^{-1}. Continuously rising intensity is observed above 2.5 μm^{-1} which does not peak below the experimental limit. [d] Band maxima and molar absorptivities of $[Ru_2(O_2CCH_3)_4]Cl$ in aqueous solution (ref 24), from 0.8 to 3.3 μm^{-1}. Continuously rising intensity is observed above 2.7 μm^{-1} which does not peak below the experimental limit.

Table VI. Electronic Spectra of $Rh_2(O_2CR)_4(H_2O)_2^{0,+}$ (μm^{-1})

D_{2h} transition	type[a]	Calcd,[b] $Rh_2(O_2CH)_4(H_2O)_2$	exptl,[c] $Rh_2(O_2CCH_3)_4(H_2O)_2$	calcd,[b] $Rh_2(O_2CH)_4(H_2O)_2^+$	exptl,[d] $Rh_2(O_2CCH_3)_4(H_2O)_2^+$
$8a_g \rightarrow 7b_{1u}$	$\delta \rightarrow \delta^*$			0.92	1.32 (ϵ 308)
$5b_{2g}, 4b_{3g} \rightarrow 7b_{1u}$	O $\rightarrow \delta^*$			1.63	
$4b_{2g}, 3b_{3g} \rightarrow 7b_{1u}$	O $\rightarrow \delta^*$			1.93	
$6b_{3g}, 6b_{2g} \rightarrow 8b_{1u}$	$\pi^* \rightarrow \sigma^*$	1.97	1.71 (ϵ 241)	2.28	1.94 (ϵ 298)
$6b_{3g}, 6b_{2g} \rightarrow 5a_{1u}$	$\pi^* \rightarrow$ Rh–O σ^*	2.47	2.27 (ϵ 106)	2.68	~2.5[e]

[a] δ, δ^*, π^*, and σ^* denote the Rh–Rh character of mainly Rh orbitals. O denotes a mainly formate-oxygen lone pair orbital. Rh–O σ^* is a mainly Rh orbital of δ^* symmetry with respect to the Rh–Rh bond. [b] All spin- and D_{4h} symmetry dipole-allowed transitions between 0.5 and 2.8 μm^{-1} except $5b_{3g} \rightarrow 7b_{1u}$ ($H_2O\pi \rightarrow \delta^*$) for the cation, calculated ca. 1.1 μm^{-1}, which should be extremely weak due to poor orbital overlap. From spin-polarized transition-state calculations. Average energies are quoted where the lower orbital is either b_{2g} or b_{3g}. [c] Band maxima and molar absorptivities in aqueous solution, from ref 24. [d] Band maxima and molar absorptivities in 1 M CF_3SO_3H, from ref 24. [e] See Figure 2 in ref 25.

weaken, than the $Rh^{2.5+}$–$Rh^{2.5+}$ bond. Thus, both the approximate interaction diagram and the quantitative calculations suggest that Cl^- is *intrinsically* a better M–M weakening trans ligand than H_2O. At the time of this writing, the first experimental data which directly tests this hypothesis has just been obtained, namely, the comparative structures of $Ru_2(O_2CR)_4(H_2O)_2^+$ and $Ru_2(O_2CR)_4Cl_{1,2}^{0,-}$ (see **1** above).[14b] The Ru–Ru bond in the aquo complex is indeed shorter than the average for the chloro complexes, by 0.035 Å.

2 suggests two second-order differences between Cl^- and H_2O as trans ligands which are confirmed by the quantitative calculations. First, H_2O introduces M–M σ^* character into the filled orbitals at lower energies on the average than Cl^-, as confirmed by Figure 4. Second, M–M σ character shifts to lower average energies in the presence of trans Cl^- than trans H_2O, as confirmed by Figure 3. Both effects favor H_2O over Cl^- as a trans bond weakener, but they should be much less important than the first-order donation into the M–M σ^* orbital.

Finally, we note that the higher relative Cl^- lone pair energies result in the middle of the three orbitals in both symmetries being most important for Ru–Cl bonding, while the lowest is most important for Rh–OH_2 bonding (see Figures 3 and 4). This is reflected in the labels on the energy levels in Figures 1 and 2.

$Rh_2(O_2CR)_4(H_2O)_2^+$ vs. $Rh_2(O_2CR)_4(H_2O)_2$. It is interesting to consider the effect of increased metal oxidation state on the axial L–M–M–L bonding. We believe that the observed structural differences between $Rh_2(O_2CCH_3)_4(H_2O)_2$ and $[Rh_2(O_2CCH_3)_4(H_2O)_2]ClO_4 \cdot H_2O$[15ac] are consistent with our calculated electronic structures. The observations are that the Rh–Rh, Rh–OH_2, and Rh–O(acetate) distances are respectively 0.069 (2), 0.089 (10), and 0.025 (9) Å shorter in the cationic than in the neutral complex. The simple effects of *normal* bond strengthening and Rh covalent radius contraction due to the increased Rh positive charge may be approximately accounted for by subtracting the Rh–O(acetate) shortening *twice* from the Rh–Rh and *once* from the Rh–OH_2 shortening. This leaves ΔRh–Rh = −0.02 Å and ΔRh–OH_2 = 0.06 Å from neutral complex to ion.

We see the extra 0.06 Å Rh–OH_2 shortening as due to the fact that the Rh–OH_2 bond starts out so much weaker than the Rh–O(acetate) bond (in $Rh_2(O_2CCH_3)_4(H_2O)_2$, the Rh–OH_2 distance is 0.27 Å longer than the average Rh–O(acetate) distance.[15a] Bond distances are well-known to become rapidly more sensitive to bond strength as the bond strength decreases.[32] The fact that the Rh–Rh distance still *decreases* slightly in the face of the Rh–OH_2 shortening testifies to the weakness of the Rh–OH_2 interaction. The amount of Rh–Rh bond strength lost to the Rh–OH_2 bond upon oxidation is apparently less than the small amount gained by removal of the δ^* antibonding electron.

These ideas are explicitly confirmed by comparison of wave function contour maps for $Rh_2(O_2CH)_4(H_2O)_2$ and $Rh_2(O_2CH)_4(H_2O)_2^+$. Of particular importance are the maps of the $4b_{1u}$ orbital (Figure 4 here and in ref 5), the key orbital for both Rh–OH_2 bonding and resulting Rh–Rh bond weakening. The increased Rh–OH_2 bonding overlap from neutral complex to ion is easily seen, but there is no comparable increase in Rh–Rh antibonding character.

$Rh_2(O_2CCH_3)_4L_2$, L = H_2O, py, $NHEt_2$, CO, PF_3, $P(OPh)_3$,

PPh_3, $P(OMe)_3$. In a recent paper,[15b] Christoph and Koh (hereafter CK) report the molecular structures of these complexes and use the variation in Rh–Rh distance along the series (from 2.39 to 2.46 Å) to develop ideas about the electronic structures which differ somewhat from our own. They see the ordering of Rh–Rh distances as requiring significant back-donation to CO and PR_3 from a high-lying orbital of e_u (i.e., Rh–Rh π) rather than e_g (i.e., Rh–Rh π^*) symmetry. They believe that placement of the π^* orbitals above the π in energy—the intuitively expected ordering, and that found by our calculations—would require that Rh→L π bonding be negligible and that the Rh–L σ overlaps for H_2O, py, and $NHEt_2$ decrease significantly faster with distance than for CO and PR_3. They recognize the weight of evidence for a single Rh–Rh bond in the carboxylate dimers from electronic spectra, ESR spectra, analogies with other compounds, and calculations.[5,33] This leads them to propose an energy level diagram with both π^* and π orbitals filled, but with π higher than π^* in energy.

We believe that the structural data of CK are consistent, rather than inconsistent, with our calculated electronic structures, in particular with the ordering $\pi < \pi^*$. Our basic hypothesis is that the order of increasing Rh–Rh distance is the order of increasing Rh–L σ covalent bond strength. We agree with CK that nonnegligible Rh→L π donation is present for L = CO and PR_3, but we believe that (1) this donation comes from the π^* rather than the π orbitals; (2) at the extremely long Rh–L distances in these compounds (averaging 0.22 Å longer than normal), the Lσ→Rh–Rh σ^* donation is stronger than the π back-donation for all ligands, and stronger for L = CO and PR_3 than for L = H_2O, py, and $NHEt_2$. We now present arguments supporting our view.

The very existence of the Rh–Rh bond requires that the Rh–Rh π^* orbitals have more π donor ability, and the Rh–Rh π orbitals less, than normal. The π bonding orbital will have charge concentrated between the metals, and thus away from the axial ligands, while its antibonding counterpart will have charge projected toward the ligands. Drago et al.[34] have demonstrated the back-bonding capability of $Rh_2(O_2CC_3H_7)_4$ by measuring ΔH_f of $Rh_2(O_2CC_3H_7)_4L_2$ in solution. They are able to separate out a "σ only" component of ΔH_f using E and C parameters, and thus determine when a significant π component is present. Even for L = py, not normally a π acceptor, some extra stabilization over the "σ only" ΔH_f is found. As they point out, the reasonable explanation for this enhanced donating ability of the rhodium carboxylate dimers is the hybridization of the Rh–Rh π^* orbital toward the ligands due to the Rh–Rh bonding.

As CK emphasize, the magnitude of a donor–acceptor interaction is proportional to $S^2/\Delta E$, where S is the overlap and ΔE is the energy separation of the interacting orbitals. The overlap factor clearly favors Rh–Rh π^* over Rh–Rh π for donation to Lπ acceptor orbitals. Likewise, Rh–Rh bonding by itself will give π^* the more favorable ΔE by establishing the energy order $\pi < \pi^*$. The specific requirement for π to become the donor orbital of choice is thus that it interact so much more strongly with *carboxylate* orbitals than does π^* that the overlap factor and ΔE established by Rh–Rh bonding are completely overwhelmed. We find nothing in either our qualitative analysis or quantitative calculations of Rh_2^{4+}, HCO_2^-, or the complexes to suggest that such a dramatic effect should or does exist.

Our conclusion that the Rh→L π donation in these complexes involves the π^* orbital leads to the further deduction that the ordering of Rh–Rh distances is determined by the Rh←L σ rather than Rh→L π interactions. If the π interaction were dominant, surely $Rh_2(O_2CCH_3)_4(CO)_2$ would have a shorter, rather than 0.034 Å longer, Rh–Rh distance than $Rh_2(O_2CCH_3)_4(H_2O)_2$. Moreover, as emphasized by CK themselves in their Figures 6 and 7, Rh→L π bonding should decrease faster with distance than Rh←L σ bonding, and we are dealing with Rh–L distances averaging 0.22 Å longer than normal. Finally, for the two ligands studied by both Drago et al.[34] and CK,[15b] py and $P(OR)_3$, the former authors find the "σ only" ΔH_f to be about 70% of the total.

We believe that it is quite reasonable for the σ covalent components of these long Rh–L bonds to be stronger for CO and PR_3 than for H_2O, py, and Et_2NH. Considering the σ bond strength in terms of $S^2/\Delta E$, the ionization energies of the Lσ lone pairs (and hence, presumably, ΔE with the Rh–Rh σ^* orbital) decrease in the order $H_2O > CO > PF_3 > py > P(OMe)_3 > Et_2NH > PPh_3$. Hence the ordering the Rh–Rh distances *is* essentially the inverse of the ΔE ordering, except that the trans influences of py and Et_2NH are smaller than expected. We believe that this reflects the importance of the overlap factor; that, at the long Rh–L distances present, the more diffuse lone pairs of CO and PR_3 overlap more effectively with the Rh–Rh σ^* function than do the rather compact lone pairs of H_2O, py, and Et_2NH.

CK cite literature Rh–L S^2 values[35] to support their view that the values of $S^2/\Delta E$ for the Rh–L σ interaction do not increase in the order of the observed Rh–Rh distances. There are several problems with these S^2 values. They were calculated at normal Rh–L distances, 0.22 Å shorter on the average than these in the complexes in question. They were calculated assuming Rh^+, probably too high a charge; our calculations on $Rh_2(O_2CH)_4$ indicate about $Rh^{0.25+}$. Most seriously, they were calculated assuming a pure Rh 5p atomic function as the acceptor orbital. The 5p orbitals are much more diffuse than the 4d orbitals which almost certainly compose most of the Rh–Rh σ^* orbital; our calculations indicate that this orbital is about 92% d_{z^2}, 5% s, and 3% p_z. The 5p-based S^2 values will consequently be much less sensitive to L and the Rh–L distance than in the real situation. In other words, we do not see the literature S^2 values as very relevant to the question of how strongly axial ligands interact with the orbitally complex Rh–Rh bond, with its myriad of possibilities for hybridization, and rehybridization upon interaction. We plan to explicitly calculate $Rh_2(O_2CH)_4L_2$, L = CO, PH_3, in hopes of characterizing the L–Rh–Rh–L bonding in detail.

Electronic Spectra of $Ru_2(O_2CR)_4^+$ Complexes. The visible diffuse reflectance spectrum[26] of solid $Ru_2(O_2CCH_3)_4Cl$ shows a single prominent band with a primary maximum at 2.16 μm^{-1} and a secondary maximum at 1.79 μm^{-1}. In aqueous solution, $Ru_2(O_2CCH_3)_4Cl$ is a 1:1 electrolyte,[21a] and the reported spectrum there[21a,24] is therefore almost certainly that of $Ru_2(O_2CCH_3)_4(H_2O)_2^+$. Like the solid-state spectrum, it contains a single prominent band, now with a single maximum at 2.36 μm^{-1}. As indicated in Table V, we assign this band in both the solid state and solution to an allowed Oπ→π^* transition, where the "Oπ" orbital is a mainly Ru–O bonding orbital with a significant Ru–Ru π bonding contribution. A possible explanation for the splitting into two components in the solid is lifting of the π and π^* orbital degeneracies by the low site symmetry of the crystal. Our calculated energy (1.99 μm^{-1}) is essentially the average energy of the two experimental maxima (1.96 μm^{-1}). Another possibility is that the 1.79-μm^{-1} maximum is due to a Cl→π^* or Cl→δ^* transition (see Table V).

The prominent visible band was originally assigned as $\delta \rightarrow \sigma_n$,[14a,24] but, as indicated earlier, the σ_n orbitals are now generally believed not to exist in the proper energy range. Moreover, resonance Raman experiments have shown that the band corresponds to a dipole allowed transition,[26] which $\delta \rightarrow \sigma_n$ ($b_{2g} \rightarrow a_{1g}, a_{2u}$) is not. The investigators of the Raman spectrum proposed a $\delta \rightarrow \delta^*$ assignment. Our calculations indicate that the $\delta \rightarrow \delta^*$ transition lies at much lower energy. The $\delta^2\delta^{*1}$ configuration is one for which previous experience indicates

that the $\delta \rightarrow \delta^*$ transition should be calculated accurately, in contrast to the low theoretical values for $\delta^2\delta^{*0}$ configurations.[20,36,37] Our predicted $\delta \rightarrow \delta^*$ energy lies outside the experimental range for the solid-state spectrum of $Ru_2(O_2CCH_3)_4Cl$, but it is close to the energy of a weak band in the solution spectrum, which we thus assign to $\delta \rightarrow \delta^*$ (see Table V). The authors report that this band is actually composite, with two maxima. A forbidden transition, $\delta \rightarrow \pi^*$, is predicted close to $\delta \rightarrow \delta^*$, and we suggest that it may contribute to the observed intensity. Even in quadruply bonded dimers $\delta \rightarrow \delta^*$ transitions are fairly weak, and it is perhaps not surprising that, at the longer metal–metal distance in the Ru(2.5) complexes, their intensity should be comparable to that of forbidden transitions.

Above 2.3 μm^{-1} the calculations predict a very large number of allowed transitions. The first few are listed in Table V. This is consistent with the experimental solution spectrum,[21a] which shows intense absorption (reaching $\epsilon > 2000$) in the range 2.5–5.0 μm^{-1} that appears to be due to a number of overlapping transitions. We make no attempt to assign this complicated region of the spectrum.

Electronic Spectra of $Rh_2(O_2CR)_4^{0,+}$ Complexes. In our previous paper on Rh(II) carboxylate dimers,[5] we assigned the two bands in the visible solution spectra of $Rh_2(O_2CR)_4L_2$ to allowed $\pi^* \rightarrow \sigma^*$ and $\pi^* \rightarrow$ Rh–O σ^* transitions. The assignment was based on the close match between calculated and experimental energies, and the observed shifts in band energies with varying L. We have since completed explicit spin-polarized transition-state calculations of the excitation energies, which are compared with experiment in Table VI. Our assignment has recently received support from single-crystal polarized spectra of $Rh_2(O_2CCH_3)_4(H_2O)_2$.[33,38] The 1.7- and 2.3-μm^{-1} bands are found to be largely xy polarized, as predicted by the calculations. For each band a weaker z-polarized component appears at slightly lower energies than the xy-polarized maximum. Since the δ^* orbital lies just above the π^* orbital in our calculation, reasonable assignments for these z components are forbidden $\delta^* \rightarrow \sigma^*$ ($7b_{1u} \rightarrow 8b_{1u}$) and $\delta^* \rightarrow$ Rh–O σ^* ($7b_{1u} \rightarrow 5a_u$) transitions, respectively, the intensity coming from a vibronic mechanism. Another reasonable possibility for the 2.3-μm^{-1} z component, which is the more prominent, is a $\delta \rightarrow \sigma^*$ ($9a_g \rightarrow 8b_{1u}$) transition. This excitation, uniquely among those below 3.0 μm^{-1}, is forbidden in D_{4h}, but allowed in D_{2h} in the z direction.

The solution spectrum of $Rh_2(O_2CCH_3)_4(H_2O)_2^+$ contains two bands completely analogous to those observed for the neutral species, but shifted to slightly higher energies.[24,25] This is in accord with the comparative orbital and excitation energies calculated for $Rh_2(O_2CH)_4(H_2O)_2$ and $Rh_2(O_2CH)_4(H_2O)_2^+$, as shown in Figure 2 and Table VI. As a result of the upward energy shift, the band assigned to $\pi^* \rightarrow$ Rh–O σ^* passes under the envelope of higher energy, higher intensity transitions in some solvents. The qualitative difference between the visible spectra of the cation and neutral species is the appearance of a new low-energy band near 1.3 μm^{-1} for the former. As indicated in Table VI, our calculations suggest a $\delta \rightarrow \delta^*$ assignment for this band. We cannot entirely exclude an O $\rightarrow \delta^*$ charge transfer assignment. The $\delta \rightarrow \delta^*$ transition would be z polarized, and the O $\rightarrow \delta^*$ xy polarized; thus single crystal polarized spectra could settle this question.

ESR Spectra of $Ru_2(O_2CR)_4^+$ Complexes. The frozen-solution ESR spectrum of $Ru_2(O_2CC_3H_7)_4Cl$ has been reported by Cotton and Pedersen.[23] Here we compare it with predictions from the present calculations. The discussion will be only qualitative, because of the large number of excited states which contribute, and because of significant experimental uncertainties in the spin Hamiltonian parameters. Nevertheless, we can show that the spectrum is at least consistent with the calculated electronic structure.

The experimental spectrum can be analyzed in terms of a tetragonal spin Hamiltonian

$$H = \mu[g_\parallel H_z S_z + g_\perp (H_x S_x + H_y S_y)] + D[S_z^2 - S(S+1)/3] + E(S_x^2 - S_y^2) + A_\parallel S_z I_z + A_\perp (S_x I_x + S_y I_y) \quad (1)$$

where $S = {}^3/_2$ and we consider the most likely mixture of Ru isotopes,[23] in which one nucleus is ^{99}Ru or ^{101}Ru, with $I = {}^5/_2$, and the other is ^{96}Ru, ^{98}Ru, ^{100}Ru, ^{102}Ru, or ^{104}Ru, with $I = 0$. The zero field splitting is sufficiently large ($|2D| > 2.2$ cm^{-1}) so that only the $M_s = -{}^1/_2 \rightarrow M_s = {}^1/_2$ transition is observed. Computer simulation of the 4.2 K spectrum yields the parameters $g_\perp = 2.18$ and $A_\perp = 3.1 \times 10^{-3}$ cm^{-1}. Less precisely determined are $g_\parallel = 2.1 \pm 0.1$ and $|A_\parallel| = (9 \pm 3) \times 10^{-3}$ cm^{-1}. The observed intensity pattern is inconsistent with a trapped-valence state in which the spin is localized at one of the ruthenium nuclei in the dimers.[23]

The theoretical expression for the g tensor, expanded through second order in perturbation theory, has the following general form:[39]

$$g_{zz} = 2 + \frac{1}{S} \sum_{n,p} \sum_{k} \frac{\langle \psi_p | l_k^z | \psi_n \rangle \langle \psi_n | \xi_k(r_k) l_k^z | \psi_p \rangle}{\epsilon_p - \epsilon_n} \quad (2)$$

Here ψ_p is any orbital that contains an odd electron, ψ_n is any orbital which is either full or empty, and ϵ_p and ϵ_n are the corresponding orbital energies. The sum over k is over all atoms in the molecule, with spin–orbit coupling constants ξ_k. In a crystal-field model, only the ruthenium nuclei would contribute. The orbital energy difference $\epsilon_p - \epsilon_n$ may be replaced for greater accuracy by a transition-state estimate of the state energy difference. There are corresponding expressions for g_{xx} and g_{yy}.

The angular momentum operator transforms in D_{4h} as $e_g + a_{2g}$, so that symmetry considerations limit the number of excited states that need to be considered in eq 2. Consider, for example, the contributions to $\Delta g_\parallel$. In the crystal-field model, the only excited state that enters here is the promotion from the half-filled $2b_{1u}$ (Ru–Ru δ^*) orbital to the $4b_{2u}$ (Ru–O σ^*) unoccupied orbital. This corresponds to an excitation from an orbital with d_{xy} character to one with character $d_{x^2-y^2}$, both orbitals having odd inversion symmetry. If this were the only excited state of importance, one would expect $g_\parallel < 2$, in line with the general rule that excited states formed by promoting an unpaired electron into an empty orbital give a negative contribution to the g-tensor element, reducing it from the free-spin value. The Xα–SW calculation, however, shows two additional *occupied* orbitals of b_{2u} symmetry that contain significant ruthenium $d_{x^2-y^2}$ character: the $2b_{2u}$ and $3b_{2u}$ have 17 and 20% metal d character, respectively. Excitations from these orbitals into the $2b_{1u}$ (δ^*) orbital will lead to positive g-tensor shifts. The observed value of $g_\parallel$ will contain contributions from all three of these excited states.

We can follow common procedures[40] in an attempt to obtain a more quantitative estimate of these effects. We write the $2b_{1u}$ (δ^*) molecular orbital in the form

$$|2b_{1u}\rangle = \frac{\alpha}{\sqrt{2}} (d_{xy}^A - d_{xy}^B) + \text{ligand contributions} \quad (3)$$

where A and B label the ruthenium nuclei, and α is an effective covalency parameter. In the muffin-tin model, α^2 gives the fraction of metal d character in this orbital.[28] In a similar fashion we write

$$|nb_{2u}\rangle = \frac{\beta_n}{\sqrt{2}} (d_{x^2-y^2}^A - d_{x^2-y^2}^B) + \text{ligand contributions} \quad (4)$$

where $n = 2$, 3, and 4. Values for α and β_n are collected in

Table VII. Calculation of $g_\parallel$ for $Ru_2(O_2CH)_4Cl_2^-$

orbital	% Ru d character	ϵ^a	$\Delta_n{}^b$	$\Delta g_\parallel{}^c$
$2b_{1u}$	$0.71 \equiv \alpha^2$	−0.221		
$2b_{2u}$	$0.17 \equiv (\beta_2)^2$	−0.591	81 300	0.003
$3b_{2u}$	$0.20 \equiv (\beta_3)^2$	−0.369	32 400	0.010
$4b_{2u}$	$0.67 \equiv (\beta_4)^2$	−0.99	26 800	−0.042
			net	−0.029

[a] Orbital energy in hartrees. [b] $\Delta_n \equiv \epsilon(2b_{1u}) - \epsilon(nb_{2u})$, in cm^{-1}. [c] Calculated from eq 6, assuming λ 880 cm^{-1}, a value between the atomic values for Ru^0 (878 cm^{-1}) and Ru^+ (887 cm^{-1}). The calculations predict ca. $Ru^{0.4+}$.

Table VII, along with the corresponding orbital energies.

The matrix elements that appear in eq 2 can be evaluated by the approximate procedure suggested by Stone,[39] e.g.

$$\langle 2b_{1u}|l_A{}^Z + l_B{}^Z|2b_{2u}\rangle \approx \frac{\alpha\beta_2}{2}\langle d_{xy}{}^A|l_A{}^Z|d_{x^2-y^2}{}^A\rangle + \frac{\alpha\beta_2}{2}\langle d_{xy}{}^B|l_B{}^Z|d_{x^2-y^2}{}^B\rangle = 2i\alpha\beta_2 \quad (5)$$

Proceeding in this fashion we find

$$g_\parallel = 2 + \frac{4\lambda\alpha^2}{S}\left\{\frac{\beta_2{}^2}{\Delta_2} + \frac{\beta_3{}^2}{\Delta_3} - \frac{\beta_4{}^2}{\Delta_4}\right\} \quad (6)$$

where $\Delta_n \equiv |\epsilon(2b_{1u}) - \epsilon(nb_{2u})|$ for $n = 2, 3, 4$, and λ is the spin–orbit coupling constant for Ru, i.e., the integral of $\xi(r)$ over the radial part of the d orbital. The three contributions to $g_\parallel$ are also given in Table I. The net result is a small negative shift, which is probably within the experimental uncertainty of the small positive shift found in the computer simulation of the experimental spectrum.[23]

The calculation of $g_\perp$ is still more complex because there are more excited states with the proper symmetry to contribute to the deviation from the free-spin value. The *most* important crystal-field-like excitation appears to be $2b_{2g}(\delta) \rightarrow 6e_g(\pi^*)$, which has a calculated excitation energy $\Delta \simeq 8700$ cm^{-1}. There is a also a lower lying $1b_{2g}$ orbital with significant Ru d character that would also contribute. A second set of contributions comes from $5e_u$, $6e_u$, $7e_u$ (all π character)$\rightarrow 2b_{1u}(\delta^*)$. Yet another set is $5a_{1g}$, $6a_{1g}$, $7a_{1g}$ (d_{z^2} or σ-bonding character)$\rightarrow 6e_g(\pi^*)$. All of these correspond to excitations into a partially filled orbital, and hence lead to positive g-tensor shifts. The only crystal-field-like excitation that can lead to a negative shift is $6e_g(\pi^*) \rightarrow 5b_{1g}$ (Ru–O σ^*), and this will be balanced in part by the promotion $4b_{1g} \rightarrow 6e_g$ with a positive shift. Thus the observed positive g-tensor shift is completely consistent with the electronic structure proposed here. If we adopt the approximations listed above for $g_\parallel$, the ten excited states listed here combine to give $g_\perp = 2.18$, in excellent agreement with the observed value.[23]

It may be prudent at this point to list some of the uncertainties in the present calculation, in order to indicate why such results should be viewed as semiquantitative at best. Aside from intrinsic inaccuracies in the Xα–SW model, there are at least three additional possible sources of error. (1) State energy differences may not be well approximated by orbital energy differences. While in the present case this could be improved by transition-state calculations, such results are unlikely to have an absolute accuracy better than about 4000 cm^{-1}, and uncertainties of this magnitude can be important in a quantitative calculation. (2) Our treatment of covalency effects has been quite crude. A more correct version would recognize that covalency affects the spin–orbit and orbital Zeeman matrix elements of eq 2 in different ways.[28,41] Further, the use of a single spin–orbit coupling constant to represent all orbitals is a serious limitation.[28,41-43] While it is feasible in the scattered-wave model to handle covalency in a more correct fashion,[28] not all of the error can be removed; in view of the additional experimental and theoretical uncertainties for the present case, such calculations do not seem warranted. (3) Contributions to the g tensor in third order in perturbation theory will arise from doublets as well as quartet states.[44] Since some of these may have excitation energies below those of the quartet states considered above, it is not clear that third-order contributions may safely be ignored.

It is worth noting that these difficulties are not unique to a molecular orbital or Xα approach, but must be faced even by possibly more accurate ab initio calculations.[45] It does not seem likely that any current method could quantitatively predict the behavior of systems as large as this one in an a priori fashion.

We consider next the hyperfine structure due to the ruthenium nuclear spin, and organize our discussion around the various terms that enter in perturbation theory. Two terms enter in first order. One is the Fermi contact term, related to the spin density at the ruthenium nucleus. In the spin restricted theory this term vanishes, because the unpaired electrons are in d-like molecular orbitals. Spin polarization effects can lead to a finite spin density at the nucleus. In the present spin unrestricted calculation

$$\rho^{spin}(0) \equiv \sum_\alpha \psi_i{}^2(0) - \sum_\beta \psi_i{}^2(0) = -0.403 a_0{}^{-3} \quad (7)$$

This corresponds to a hyperfine coupling constant for ^{99}Ru of

$$a_{Ru} = \left(\frac{4\pi}{3M_s}\right) g_e\beta_e g_N\beta_N \rho^{spin}(0) \simeq 9 \times 10^{-4}\ cm^{-1} \quad (8)$$

We have no good way of estimating the probable error in this number. Xα calculations on first-row transition-metal complexes show that this sort of calculation often underestimates the extent of s-orbital polarization.[28,46] Comparable studies are not available for heavier elements, but it seems likely that the estimate in eq 7 and 8 is also an underestimate, perhaps by 100% or more.

A dipolar term also contributes in first order, with the perturbation expression

$$A_{xx}{}^\circ = \frac{g_e\beta_e g_N\beta_N}{M_s}\sum_i \left\langle \frac{3(r_x{}^i)^2 - (r^i)^2}{(r^i)^5}\hat{S}_z{}^i \right\rangle \quad (9)$$

where r^i is the position of the ith electron and $S_z{}^i$ is the z component of its spin operator. In the present case the spin distribution around each Ru nucleus is the sum of d_{xy}, d_{xz}, and d_{yz}-like orbitals, the net spin distribution being nearly spherically symmetric. This leads to very small first-order dipolar contributions for both the spin-restricted and unrestricted calculations, $A_\parallel{}^\circ = -2A_\perp{}^\circ \simeq -0.6 \times 10^{-4}$ cm^{-1}.

Second-order contributions to the hyperfine tensor can conveniently be divided into three parts.[47] The first involves an interaction between the orbital moment of the electron and the nuclear magnetic moment, which leads to a contribution proportional to the deviation of the g tensor from its spin-only value; e.g.

$$\Lambda_\perp{}' = g_e\beta_e g_N\beta_N\langle r^{-3}\rangle(g_\perp - 2) \quad (10)$$

As with the g tensor, only excited states of the same multiplicity as the ground state contribute. The notation Λ' follows Maki and McGarvey,[48] and $\langle r^{-3}\rangle$ is a radial expectation value of the inverse cube of the distance of the electron in an unpaired orbital from one of the Ru nuclei. For the metal–metal dimer case, this should be roughly half the value of a ruthenium 4d atomic orbital, which is about $6a_0{}^{-3}$. With this estimate Λ_p'

is $\sim -4 \times 10^{-4}$ cm^{-1}. Since this is an order of magnitude smaller than the observed hyperfine tensors, it is clear that a more precise estimate is not of qualitative significance.

Other second-order terms arise from the interaction of the nuclear magnetic moment with the spin moment of the electron.[40] Contributions of this sort from excited quartet states are similar in magnitude to the tensor Λ' discussed above, and cannot be used to rationalize in a simple way the qualitative hyperfine behavior. Doublet states of the form $(\pi_x^*)^2(\delta^*)$ or $(\pi_y^*)^2(\delta^*)$ can mix with the ground state via spin–orbit coupling, but these states do not contribute in second order since matrix elements of the form ⟨ground state|hyperfine perturbation|excited doublet⟩ vanish. Such states, because of their low excitation energies, may be important in higher orders of perturbation theory. Because dozens of terms would enter, such a calculation does not seem warranted given our present level of theoretical uncertainties.

From this qualitative discussion we can conclude that the "common" first- and second-order hyperfine effects are small for $Ru_2(O_2CH_2)_4^+$ and that the observed coupling appears to arise from a large number of second-order terms or from higher order effects. For this and similar systems, then, it will be difficult to extract detailed bonding information from the ESR spectra.

Acknowledgments. We are grateful to G. G. Christoph, R. J. H. Clark, F. A. Cotton, G. Gliemann, V. L. Goedken, and D. S. Martin for their comments and for communication of results prior to publication. We thank the National Science Foundation and the donors of the Petroleum Research Fund, administered by the American Chemical Society, for support.

Supplementary Material Available: Table I, sphere radii and SCF charge distributions (1 page). Ordering information is given on any current masthead page.

References and Notes

(1) (a) University of Washington; (b) University of California.
(2) J. G. Norman, Jr., and H. J. Kolari, *J. Chem. Soc., Chem. Commun.*, 303 (1974); *J. Am. Chem. Soc.*, **97**, 33 (1975).
(3) (a) J. G. Norman, Jr., and H. J. Kolari, *J. Chem. Soc., Chem. Commun.*, 649 (1975); (b) J. G. Norman, Jr., and H. J. Kolari, H. B. Gray, and W. C. Trogler, *Inorg. Chem.*, **16**, 987 (1977).
(4) (a) J. G. Norman, Jr., and D. J. Gmur, *J. Am. Chem. Soc.*, **99**, 1446 (1977); (b) W. Klotzbücher, G. A. Ozin, J. G. Norman, Jr., and H. J. Kolari, *Inorg. Chem.*, **16**, 2871 (1977).
(5) J. G. Norman, Jr., and H. J. Kolari, *J. Am. Chem. Soc.*, **100**, 791 (1978).
(6) G. A. Ozin, H. Huber, D. McIntosh, S. Mitchell, J. G. Norman, Jr., and L. Noodleman, *J. Am. Chem. Soc.*, **101**, 3504 (1979).
(7) J. G. Norman, Jr., B. J. Kalbacher, and S. C. Jackels, *J. Chem. Soc., Commun.*, 1027 (1978).
(8) G. C. Aleksandrov and Y. T. Struchkov, *J. Organomet. Chem.*, **27**, 53 (1971); *J. Struct. Chem.*, **11**, 438 (1970).
(9) (a) F. A. Cotton, M. W. Extine, and G. W. Rice., *Inorg. Chem.*, **17**, 176 (1978); (b) F. A. Cotton and G. W. Rice, *Ibid.*, **17**, 688, 2004 (1978); and references cited therein.
(10) J. Drew, M. B. Hursthouse, P. Thornton, and A. J. Welch, *J. Chem. Soc., Chem. Commun.*, 52 (1978).
(11) R. J. Doedens, *Prog. Inorg. Chem.*, **21**, 209 (1976).
(12) F. A. Cotton, M. W. Extine, and L. D. Gage, *Inorg. Chem.*, **17**, 172 (1978), and references cited therein.
(13) F. A. Cotton and L. D. Gage, *Nouveau J. Chim.*, **1**, 441 (1977).
(14) (a) M. J. Bennett, K. G. Caulton, and F. A. Cotton, *Inorg. Chem.*, **8**, 1 (1969); (b) A. Bino, F. A. Cotton, and T. Felthouse, *Inorg. Chem.*, submitted; F. A. Cotton, personal communication.
(15) (a) F. A. Cotton, B. G. DeBoer, M. D. LaPrade, J. R. Pipal, and D. A. Ucko, *Acta Crystallogr., Sect. B*, **27**, 1664 (1971); (b) G. G. Christoph and Y.-B. Koh, *J. Am. Chem. Soc.*, **101**, 1422 (1979); (c) J. J. Ziolkowski, M. Mosziar, and T. Glowiak, *J. Chem. Soc., Chem. Commun.*, 760 (1977).
(16) M. J. Bennett, W. K. Bratton, F. A. Cotton, and W. R. Robinson, *Inorg. Chem.*, **2**, 1570 (1970).
(17) F. A. Cotton and G. G. Stanley, *Inorg. Chem.*, **16**, 2668 (1977).
(18) M. Benard, *J. Am. Chem. Soc.*, **100**, 2354 (1978).
(19) F. A. Cotton, *Acc. Chem. Res.*, **11**, 225 (1978).
(20) W. C. Trogler and H. B. Gray, *Acc. Chem. Res.*, **11**, 232 (1978).
(21) (a) T. A. Stephenson and G. Wilkinson, *J. Inorg. Nucl. Chem.*, **28**, 2285 (1966); (b) R. W. Mitchell, A. Spencer, and G. Wilkinson, *J. Chem. Soc., Dalton Trans.*, 846 (1973).
(22) F. A. Cotton and J. G. Norman, Jr., *J. Am. Chem. Soc.*, **94**, 5697 (1972).
(23) F. A. Cotton and E. Pedersen, *Inorg. Chem.*, **14**, 388 (1975).
(24) C. R. Wilson and H. Taube, *Inorg. Chem.*, **14**, 2276 (1975).
(25) R. D. Cannon, D. B. Powell, K. Sarawek, and J. S. Stillman, *J. Chem. Soc., Chem. Commun.*, 31 (1976).
(26) R. J. H. Clark and M. R. Franks, *J. Chem. Soc., Dalton Trans.*, 1825 (1976).
(27) F. A. Cotton, personal communication.
(28) D. A. Case and M. Karplus, *Chem. Phys. Lett.*, **39**, 33 (1976); *J. Am. Chem. Soc.*, **99**, 6182 (1977).
(29) J. G. Norman, Jr., *Mol. Phys.*, **31**, 1191 (1976).
(30) R. E. Watson, *Phys. Rev.*, **14**, 1108 (1958).
(31) L. F. Warren and V. L. Goedken, *J. Chem. Soc., Chem. Commun.*, 909 (1978); V. L. Goedken, personal communication.
(32) F. A. Cotton and G. Wilkinson, "Advanced Inorganic Chemistry", 3rd ed., Wiley-Interscience, New York, 1972, p 124.
(33) D. S. Martin, Jr., T. R. Webb, G. A. Robbins, and P. E. Fanwick, *Inorg. Chem.*, **18**, 475 (1979).
(34) R. S. Drago, S. P. Tanner, R. M. Richmann, and J. R. Long, *J. Am. Chem. Soc.*, **101**, 2897 (1979).
(35) R. McWeeny, R. Mason, and A. D. C. Towl, *Discuss. Faraday Soc.*, **47**, 20 (1969).
(36) F. A. Cotton, P. E. Fanwick, L. D. Gage, B. Kalbacher, and D. S. Martin, *J. Am. Chem. Soc.*, **99**, 5642 (1977).
(37) L. Noodleman and J. G. Norman, Jr., *J. Chem. Phys.*, **70**, 4903 (1979).
(38) G. Bierek, W. Tuszynski, and G. Gliemann, *Z. Naturforsch. B*, **33**, 1095 (1978).
(39) A. J. Stone, *Proc. R. Soc. London, Ser. A*, **271**, 424 (1964).
(40) B. R. McGarvey in "Transition Metal Chemistry", Vol. 3, R. L. Carlin, Ed., Marcel Dekker, New York, 1966, p 90.
(41) A. A. Misetich and T. Buch, *J. Chem. Phys.*, **41**, 2524 (1964).
(42) A. A. Misetich and R. E. Watson, *Phys. Rev.*, **143**, 335 (1966).
(43) A. Hazony, *Phys. Rev. B*, **3**, 711 (1971).
(44) See, e.g., B. R. McGarvey, *Can. J. Chem.*, **53**, 2498 (1975).
(45) P. J. Hay, *J. Am. Chem. Soc.*, **100**, 2897 (1978).
(46) T. M. Wilson, J. W. Wood, and J. C. Slater, *Phys. Rev. A*, **2**, 620 (1970); see also P. E. Desmier, M. A. Whitehead, R. Bogdanovoc, and M. S. Gopinathan, *Mol. Phys.*, **33**, 1457 (1977).
(47) J. S. Griffith, "The Theory of Transition Metal Ions", Cambridge University Press, New York, 1961, Chapter 12.
(48) A. M. Maki and B. R. McGarvey, *J. Chem. Phys.*, **29**, 31 (1958).